ELSEVIER

Carbohydrate Research 277 (1995) 25–38

CARBOHYDRATE RESEARCH

Conformational analysis of heparin epoxide: molecular mechanics computations

D.R. Ferro [a,*], J. Gajdoš [a,1], M. Ragazzi [a], F. Ungarelli [b], S. Piani [b]

[a] *Istituto di Chimica delle Macromolecole del C.N.R, via E. Bassini 15, I-20133 Milan, Italy*
[b] *Alfa Wassermann S.p.A., Research Dept., via Ragazzi del '99 5, I-40133 Bologna, Italy*

Received 8 November 1994; accepted 15 May 1995

Abstract

The conformation of models of the epoxy-derivative of the glycosaminoglycan heparin has been studied by molecular mechanics calculations using a MM2-like force field extended with parameters for the oxirane ring. Two dimers, two trimers and several higher homologs modeling heparin epoxide were investigated, assuming the preferred $^5H_0$ ring form of 2,3-anhydro-α-L-guluronic acid residue. Two-dimensional (φ; ψ) maps of dimers showed the location of the energetically preferred conformers. Starting from the most stable dimer conformers, structures of trimers and other oligomers were derived and optimized, with an exhaustive search of the preferred sidechain conformers. The effect of solvation on conformation was analyzed using a continuum model of solvent. The present calculations indicate a significant flexibility of the heparin epoxide chain.

Keywords: Heparin; Heparin derivatives; Glycosaminoglycans; Conformational analysis; Molecular mechanics

1. Introduction

A complete understanding of the role of carbohydrates in biological systems is to a large extent dependent on the information available about the preferred conformations of these molecules and about the equilibrium mixture of their conformers in solution. Conformational analysis offers a tool which can determine all possible conformations which influence the behavior of carbohydrates. The conformational energies of saccharides are calculable, in principle, from either classical, so-called "empirical" procedures

* Corresponding author.
[1] Permanent address: Institute of Chemistry, Slovak Academy of Sciences, SK-84238 Bratislava, Slovakia.

SSDI 0008-6215(95)00205-7

(e.g. molecular mechanics; using empirical potential functions) or by quantum-mechanical procedures.

In crystals most molecules usually adopt one single conformation. However, in solution there is a mixture of conformations usually undergoing a fast interconversion, and most experimental techniques, like NMR, show only properties which are time averaged over several conformations [1]. Often, NMR spectroscopy alone does not give an unambiguous assignment of a specific conformation, but rather supplies limits for the conformations: in these cases, calculations of the allowed conformations of oligo- and poly-saccharides can allow the assignment and the interpretation of the experimental parameters. Therefore, usually only a combination of experimental and theoretical approaches is sufficient to provide the solution conformation of a saccharide.

It had been previously reported [2,3] that under alkaline conditions, heparin undergoes regio- and stereo-specific epoxidation of α-L-iduronic 2-sulfate residues. Preliminary biological studies indicated that this 2-desulfation changes the antiproliferative and anticoagulant activities. It has been suggested [4] that conformational behavior may influence the interaction with membrane proteins and therefore the biological properties of this compound.

In the preceding paper in this issue, Hricovíni et al. report their dynamic NMR studies on heparin epoxide in solution. Details on the preparation and biological significance may be found therein. The theoretical study (molecular mechanics calculations and calculation of the solvation energy) of the conformational behavior of this epoxide is the aim of the present paper.

2. Methods

Parametrization of the force field.—The first step of our investigation was to find reliable potentials for molecular mechanics calculations on compounds containing the oxirane ring. Recently Podlogar and Raber [5] extended Allinger's MM2 force field [6] to include epoxides. These authors tested the parameters with a series of epoxides, but nothing was done for the epoxy-derivatives of carbohydrates. We decided to test the parameter set on methyl 2,3-anhydro-4-deoxy-α-DL-*ribo*- and -α-DL-*lyxo*-hexopyranosides whose X-ray structure had been determined by Krajewski [7] (see Fig. 1). Allinger's program MM2(87) was first utilized for the two isolated molecules: the

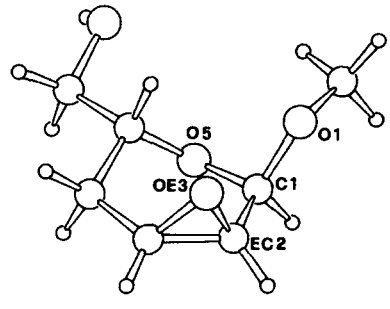

Fig. 1. Molecular structure of methyl 2,3-anhydro-4-deoxy-α-L-*ribo*-hexopyranoside (from Krajewski [7]).

Table 1
Corrections of the parameter θ_0 for bond angle EC–C–O (type 50–1–6) and corresponding changes in selected bond lengths and bond angles after MM2 and CHAMP calculation (bond angles in deg., bond lengths in Å) [a]

(i) Methyl 2,3-anhydro-4-deoxy-α-DL-*ribo*-hexopyranoside						Crystal		
θ_0	105.0	104.0	103.0	102.0	100.0	calcd [b] ($\theta_0 = 103$)		exptl
						$\epsilon = 1$	$\epsilon = 3$	
EC(2)–C(1)–O(1)	109.0	108.5	107.9	107.4	106.3	108.7	108.0	107.9
EC(2)–C(1)–O(5)	113.2	112.8	112.3	111.9	111.1	112.6	112.4	113.1
O(1)–C(1)–O(5)	109.8	110.1	110.4	110.7	111.2	106.7	110.0	112.0
C(1)–EC(2)	1.511	1.511	1.512	1.512	1.512	1.500	1.506	1.502
C(1)–O(1)	1.410	1.409	1.408	1.408	1.406	1.387	1.398	1.402
C(1)–O(5)	1.408	1.408	1.408	1.408	1.408	1.391	1.400	1.419
(ii) Methyl 2,3-anhydro-4-deoxy-β-DL-*lyxo*-hexopyranoside								
θ_0	105.0	104.0	103.0	102.0	100.0	Crystal exptl		
EC(2)–C(1)–O(1)	107.6	107.0	106.4	105.8	104.6	105.5		
EC(2)–C(1)–O(5)	113.0	112.6	112.2	111.8	111.1	112.3		
O(1)–C(1)–O(5)	108.9	109.2	109.4	109.7	110.2	112.9		
C(1)–EC(2)	1.509	1.509	1.509	1.509	1.510	1.499		
C(1)–O(1)	1.410	1.410	1.409	1.409	1.408	1.405		
C(1)–O(5)	1.410	1.410	1.410	1.409	1.409	1.410		

[a] For nomenclature, see Fig. 1.
[b] For intermolecular interactions dielectric constant 1 was used, while intramolecular interactions were calculated with $\epsilon = 1$ or 3, respectively.

default value of the dielectric constant ($\epsilon = 1.5$) was adopted, but we also performed calculations using values of ϵ in the range 1 to 4, in view of a possible modeling in the condensed phase. We found that a correction of bond angle EC–C–O (50–1–6 in MM2 type notation—angle which is formed by "epoxide" carbon–carbon–oxygen) is necessary: the value of 103° was chosen and used in the further calculations. Tests showed that it is not necessary to introduce extra parameters for the anomeric carbon. The values tried for the EC–C–O parameter, together with the values of selected bond lengths and bond angles are given in Table 1, which indicates rather good agreement between measured and computed geometry.

Solid state energy calculations.—As said, the previous calculations were done on isolated molecules. For a more realistic comparison, we transferred the corrected potentials for oxiranes from MM2 to the molecular mechanics program CHAMP(93) [8], which can deal with crystal structures (as well as with large molecular systems) more straightforwardly. As in previous works [9–11], the force field adopted here is quite close to the original MM2 potentials. Also the electronegativity correction [6] was included in the calculation: that is, a correction Δl_e to an "ideal" bond length l_0 (assigned as force field parameter) is applied whenever an electronegative (or electropositive) atom is attached to one end of that bond. Besides some differences in the treatment of hydrogen bonds [9], the only major discrepancy lies in the electrostatic

energy term, which in CHAMP(93) is computed in the monopole approximation, rather than in terms of point dipole interactions. The net atomic charges used in the calculation of the electrostactic contribution are derived directly from MM2 dipole moments, whenever available, and were taken from previous results [9,11] for the sulfate and carboxylate groups. We note that, as in such previous studies, on each of the ionic groups a net charge of $0.3e$ is taken, in order to simulate the screening of electrostatic interactions due to the counter-ions present in the solution. An effort toward a more realistic treatment, with explicit inclusion of Na^+ or K^+ ions and water molecules in the computations, is under way in our laboratory [12], but the whole set of force-field parameters was not ready for the present work.

While for a molecule in solution we assume a value of 3 for the dielectric constant, in crystal calculations, as often done in this type of computations, the dielectric constant of the medium was taken as 1 for the intermolecular interactions. However, owing to the different treatment of the Coulomb energy, since past work on simple (isolated) model compounds showed that a value of 3 for ϵ best fits the original MM2 force-field parametrization, and the choice of $\epsilon = 1$ also for nearest-neighbor interactions would lead to some distortions of the sugar ring, especially at the anomeric site, all intramolecular interactions were computed with $\epsilon = 3$. Finally, for the same reason, the bond angle parameters for O–C–O and C–O–C were modified by $+4°$ and $+2°$, respectively.

The crystal structure of methyl 2,3-anhydro-4-deoxy-α-DL-*ribo*-hexopyranoside, determined by Krajewski et al. [7], was considered in order to evaluate the ability of the present force field to reproduce not only the geometrical features, but also the molecular packing of an epoxide derivative in the solid state. The crystallographic coordinates, as well as the observed unit cell dimensions and space group ($P2_1/c$), were utilized to build the microcrystal: the positions of hydrogen atoms and lone pair pseudo-atoms were first optimized, then the total energy of the crystal was minimized with respect to the cartesian coordinates of all atoms of the asymmetric unit (here coinciding with the central molecule), keeping the cell dimensions fixed. In Table 1 the major geometrical features of the computed model are compared with the observed values. The rms deviation between computed and experimental heavy-atom coordinates is 0.23 Å, while upon best-fitting of the models by roto-translation the rms deviation (hence representing conformational discrepancies) is reduced to 0.06 Å.

Solvent effect.—In solution, the molecular energy does not depend exclusively on the arrangement of atoms in the isolated molecule, i.e. on intramolecular interactions, but also on the surrounding molecules, i.e. on intermolecular interactions, and these may differ from one conformer to another. Calculations of the effect of solvent upon the conformational energy differences in dilute solution were done with the program SOLVNT, based on a model developed by Tvaroška et al. [13,14] which was used successfully to reproduce all the known data on 2-methoxytetrahydropyran [13] and to predict solvents effects on the conformational properties of carbohydrates [15]. According to that solvophobic model [13], the total conformational free energy, ΔG, of the solute in a particular solvent is divided into the free energy of the solute molecule in the free-space approximation ΔG_{is} and the solvation free energy ΔG_{solv}

$$\Delta G = \Delta G_{is} + \Delta G_{solv}.$$

The solvation free energy, ΔG_{solv} can be partitioned into the contributions

$$\Delta G_{solv} = \Delta G_{elst} + \Delta G_{disp} + \Delta G_{cav}$$

where ΔG_{cav} is a term representing the energy required to create a cavity of sufficient size to accommodate a solute molecule in a given solvent, and ΔG_{elst} and ΔG_{disp} characterize the contribution of electrostatic and dispersion interactions of the solute molecule with the solvent. The same charge distribution has been used as for the CHAMP calculations on the isolated molecules.

As mentioned earlier, to each charged group a net charge of $0.3e$ was assigned. Thus, for example, in case of the trimer AUA the overall charge on the molecule is $1.5e$. The calculation of the solvation energy using the procedure described above can be ambiguous for charged molecules. The contribution of the electrostatic energy takes into account the dipole and quadrupole moment of the calculated system. However, for charged molecules the value of overall dipole moment is dependent on the choice of the reference system [16]. To avoid this difficulty, the origin of the coordinate system is shifted to the center of mass of the molecule; then the molecule is oriented along its principal axes of inertia. Also the quadrupole moment is calculated in translated coordinates, since it is independent of the choice of origin only if dipole and charges are zero. The electrostatic contribution also includes the so-called Born energy [17]. The interactions between ion and solvent are assumed to be electrostatic in origin, with the ion viewed as a charged sphere and the solvent as a dielectric continuum.

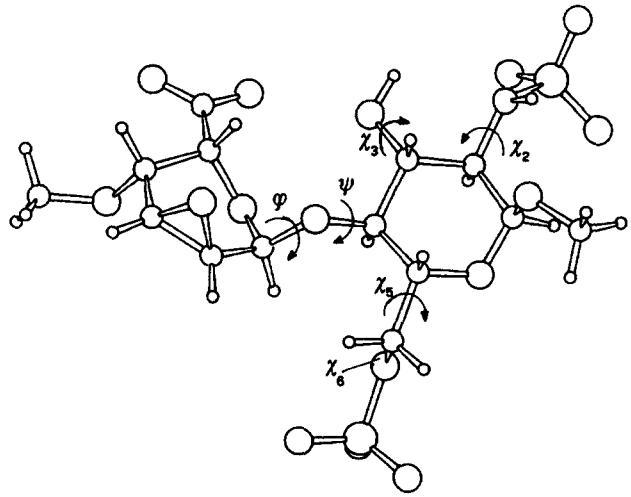

Fig. 2. The definition of the torsional angles, φ and ψ at the glycosidic linkage, and side-chain dihedrals (χ_2,χ_3,χ_5,χ_6) in the dimer building block of heparin epoxide.

3. Results and discussion

Having set as a goal the determination of the characteristics of the polymer chain, we started with the conformational study of the two dimers contained in the epoxy-heparin sequence. The calculation of (φ; ψ) maps provided the basic information about the "allowed" conformational space: this first characterization helped with the calculation of trimers whose structures were derived from the location of the dimer energy minima, and from this point we built a pentamer, and so on. For an easier description of n-mers later on, we introduced symbolic names for the residues. So, 2,3-anhydro-α-L-guluronic acid will be further referred to as residue **U**, and 2-deoxy-2-sulfomino-α-D-glucose 6-sulfate as residue **A**. A methyl group was attached on both ends of the molecules, in order to minimize the effect of free terminals. Previous calculations [18] on the ring conformation of the **U** monomer found that two conformers are allowed, namely $^5H_0$ and $^0H_5$, the former being more stable by more than 3 kcal/mol; the preference for $^5H_0$ form was confirmed in our computations, the difference (when the solvent contribution is included) being about 2 kcal/mol. On this basis, the $^0H_5$ conformer was disregarded in all the subsequent calculations.

Dimers.—There are two possible linkages for dimers, namely **AU** and **UA**. It has long been traditional in molecular mechanics studies of oligosaccharides to calculate Ramachandran-like two-dimensional contour maps of the conformational potential energy as a function of the glycosidic linkage torsional angles φ and ψ (defined as H1–C1–OG–C4′ and C1–OG–C4′–H4′; see Fig. 2). We examined the rotation about φ

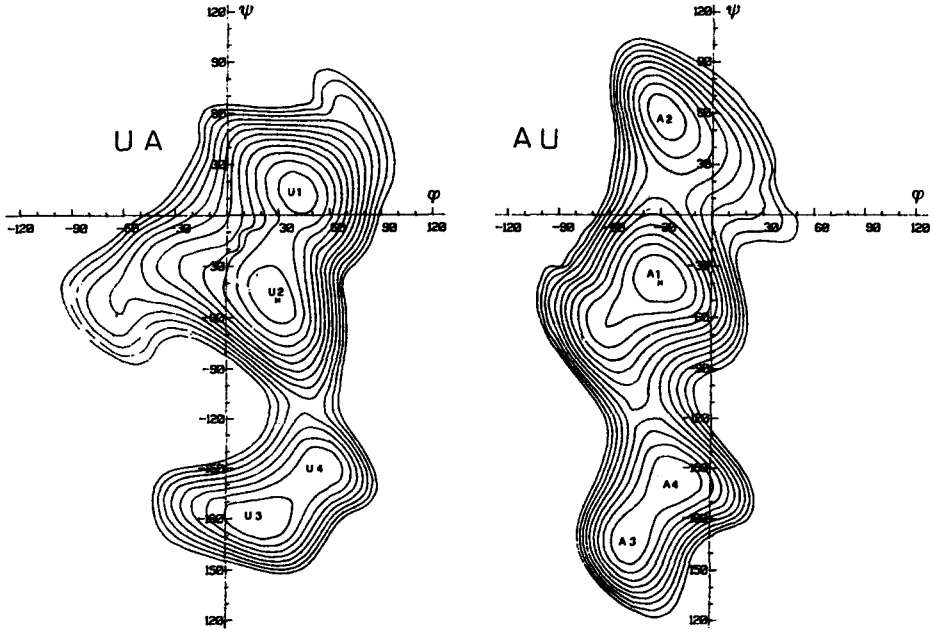

Fig. 3. Two-dimensional (φ; ψ) isoenergy contour maps (at 0.5 kcal/mol intervals) for dimers **UA** and **AU**.

Table 2
Results of conformational statistics for dimers **UA** and **AU**, at 25°C. The table shows the mean values of (φ; ψ), averaged over the domains corresponding to each state and over the sidechain conformers, together with the respective statistical weights

Dimer **UA**								
State	U1		U2		U3		U4	
	φ	ψ	φ	ψ	φ	ψ	φ	ψ
χ-Aver.	38.9	13.9	26.9	−49.7	16.1	172.7	56.1	−150.7
(rmsd)	3.2	1.3	1.1	2.6	4.0	5.2	0.9	1.8
(φ, ψ)-Aver.	39.0	11.2	25.2	−45.1	17.1	181.1	50.2	−152.7
(rmsd)	12.1	13.5	13.5	13.8	14.5	8.7	10.9	13.2
ΔE_{min}	0.166		0		1.950		2.489	
P_0 [a]	0.418		0.553		0.021		0.008	
P_1 [b]	0.422		0.568		0.008		0.002	
P_2 [c]	0.420		0.571		0.007		0.002	
Dimer **AU**								
State	A1		A2		A3		A4	
	φ	ψ	φ	ψ	φ	ψ	φ	ψ
χ-Aver.	−28.3	−38.0	−27.4	59.3	−46.7	167.4	−20.7	−157.6
(rmsd)	1.9	0.9	1.2	2.4	1.7	1.0	1.8	1.3
(φ, ψ)-Aver.	−35.5	−42.3	−24.7	53.0	−45.4	169.3	−22.9	−155.8
(rmsd)	15.6	15.1	12.2	14.7	8.7	10.8	12.0	14.0
ΔE_{min}	0		1.598		1.481		1.499	
P_0 [a]	0.814		0.055		0.067		0.064	
P_1 [b]	0.828		0.080		0.050		0.042	
P_2 [c]	0.853		0.069		0.036		0.042	

[a] Computed on the basis of energy minima (ΔE_{min}).
[b] Computed by averaging over sidechain conformers.
[c] Computed by averaging also over the (φ; ψ) domains.

and ψ angles allowing complete optimization of all degrees of freedom during rotation. The total strain energy as a function of the φ and ψ glycosidic angles (fully relaxed maps), is illustrated in Fig. 3. Such maps were computed adopting the most favorable sidechain conformation, as well as the preferred pyramidal arrangement of the C–NH–S group, for the **A** residue. A "circular driving" procedure was used to overcome discontinuities in the maps, with 5° steps for φ and ψ.

The two contour maps show four energy minima each, indicated as points U1–U4 in the case of **UA** and as A1–A4 for **AU**. For each of such points all the **A** sidechain conformers were generated and optimized (three conformational states for dihedral angles χ_2, χ_3, χ_5, and χ_6, as well as two "flips" of C–NH–S), for a statistical evaluation of the conformer populations. The results of this analysis are reported in Table 2.

Dimer **UA** presents two nearly equi-energetic (φ; ψ) minima, while other two minima, in the region of $\psi \sim 180°$, are less stable by about 2 kcal/mol, with a population of less than 1%: the presence of these conformers will be found negligible in higher oligomers. The conformer populations are little affected if they are evaluated by

Table 3
Main-chain conformer populations computed for trimer **UAU**

State	U–A		A–U		Pop.
	φ	ψ	φ	ψ	
U1 A1	40.1	14.6	−25.1	−38.8	0.476 [a] (0.511 [b])
U2 A1	23.8	−43.9	−24.5	−39.0	0.178 (0.189)
U2 A1*	23.7	−43.9	−54.6	−59.3	0.039 (0.034)
U1 A2	40.5	14.9	−26.3	60.0	0.129 (0.120)
U2 A2	25.0	−45.5	−25.4	60.0	0.041 (0.042)
U2* A2	31.1	−16.9	−25.7	57.0	0.007 (0.007)
U1 A3	40.0	14.0	−47.0	166.7	0.052 (0.044)
U2 A3	23.9	−47.8	−47.1	165.2	0.024 (0.020)
U1 A4	39.3	14.4	−23.7	−160.2	0.029 (0.021)
U2 A4	23.9	−47.4	−22.0	−159.5	0.014 (0.012)

[a] Computed by averaging over all 390 distinct conformers, which produced a few other scattered (φ; ψ) conformations accounting for 1% of the population.
[b] Computed by averaging over the 99 lowest-energy conformers, later used for **AUA**.

integration over the corresponding (φ; ψ) domains (P_2), or by accounting only for the sidechain flexibility (P_1).

In **AU**, minimum A1 is clearly favored over the other three; overall, this dimer shows a considerably lower flexibility than **UA**.

Trimers.—Starting from the (φ; ψ) minima of the dimers, the two types of trimers, **UAU** and **AUA**, were created. The combination of the four lowest-energy structures of each dimer gives 16 starting points for each trimer, which were then optimized. The distinct (φ; ψ) minima found for **UAU** were then combined, as in the case of the dimers, with all the possible sidechain conformations of **A** (including the inversion at N_2, 2×3^4 conformers for each (φ; ψ) minimum), in order to obtain a complete conformational description of the trimer. In the case of **AUA**, due to the presence of two residues carrying pendant sidechains, the same procedure would imply too many conformers. Hence a significant number of starting points was generated, on the basis of the results for **UAU**, by combining 72 conformations of the A–U linkage with 46 conformations of U–A. Such conformations are the distinct ones found in the 99 lowest-energy conformers of **UAU** (within 3 kcal/mol above the absolute minimum, accounting for about 90% of the partition function). For both trimers, all such conformations were subjected to energy minimization. The analysis of the results is summarized in Tables 3 and 4.

If one considers the main-chain conformation only, the results for the trimers suggest that the epoxy-heparin chain can be described in terms of two conformational states for the U–A glycosidic linkage and four states for the A–U linkage. If one could assume that the interactions between residues farther than next-nearest neighbors have negligible conformational effects and that such states are already well defined (including the average description of the sidechains) in the oligomers analyzed above, the populations of **AU, UA, UAU**, and **AUA** would be sufficient to determine the statistical properties of the polymer chain. Unfortunately, we found that such a hypothesis does not hold. Indeed

Table 4
Main-chain conformer populations computed for trimer **AUA**

State	A–U		U–A		Pop.	No. of conf.
	φ	ψ	φ	ψ		
A1 U1	−28.8	−37.7	39.1	13.3	0.225	102
A1* U1	−54.6	−58.5	38.1	13.2	0.002	4
A2 U1	−28.9	62.2	46.3	12.0	0.023	21
A3 U1	−48.9	160.8	38.6	15.9	0.007	9
A4 U1	−20.5	−156.3	39.7	15.1	0.004	8
A1 U2	−28.7	−38.2	27.1	−49.1	0.559	138
A1* U2	−55.5	−58.4	26.9	−49.0	0.011	15
A2 U2	−29.5	57.0	28.3	−56.0	0.119	66
A3 U2	−47.0	167.4	27.5	−50.3	0.011	11
A4 U2	−18.7	−156.2	28.6	−52.8	0.039	22

computations on a few conformers of tetramers and pentamers showed that their relative energies cannot be reproduced on the basis of the above additive rules; and it turned out that such statistics yield a conformational flexibility larger than that indicated by energy differences between conformers of 9-mers. This is partly due to long range effects of the electrostatic term, but even more to the decreasing sidechain conformational freedom when going from dimers to trimers and higher homologs. Thus, in order to to be able to extrapolate the results to the polymer chain, we resorted to some computations, necessarily less exhaustive than the previous ones, on longer chains.

Pentamer.—We used a strategy similar to the one used for **AUA** for computing the stable conformers of **UAUAU**, for the purpose of evaluating the conformer populations at its central A–U–A linkages. From the analysis of **UAU**, 54 low-energy conformers were chosen, using a somewhat higher threshold for the less stable (φ; ψ) states, and were combined to form 54×54 initial structures of **UAUAU**. The results of these energy minimizations were then analyzed and are reported in Table 5.

Heptamer.—Since the sidechain populations on the two **A** residues in Table 5 show significant differences, it appears that the central A–U–A sequence of the pentamer is not yet truely representative of the internal residues of the polymer chain. Hence the calculations were extended to heptamer **UAUAUAU**, again considering 54 conformational states for the central U–A–U linkages, but only four representative states for each of the two lateral U–A–U linkages. As the populations computed for the central (φ; ψ) states are little affected when partial subsets of the lateral states are used, we may conclude that such populations represent a good approximation to the conformational characteristics of the epoxy-heparin chain, of course within the limits of the present force field.

Moreover, these populations, summarized in Table 6, are consistent with the results of many energy minimizations carried on random conformers of the 9-mer; the six lowest-energy structures (those within 2 kcal/mol) have all A–U linkages as A1, whereas among the 24 U–A links, U2 is represented four times near the A–U tail and three times in the central region (probability 0.125 against 0.102)

A comparison among the conformer populations computed for the various oligomers

Table 5
Conformer populations in pentamer **UAUAU**

Main chain							
U1–A2				A2–U3			
State	φ	ψ	Pop.	State	φ	ψ	Pop.
1	40.7 (3.1)	14.9 (1.9)	0.874	1	−27.0 (1.9)	−38.1 (0.9)	0.910
2	22.0 (2.0)	−41.5 (2.3)	0.126	2	−23.8 (2.4)	56.0 (3.3)	0.018
				3	−47.0 (1.4)	165.9 (3.6)	0.035
				4	−21.9 (1.5)	−157.6 (1.0)	0.037
U3–A4				A4–U5			
State	φ	ψ	Pop.	State	φ	ψ	Pop.
1	38.6 (2.6)	14.5 (1.3)	0.581	1	−23.9 (2.0)	−39.2 (1.3)	0.668
2	23.6 (1.3)	−44.4 (1.8)	0.419	2	−24.9 (0.9)	61.1 (2.0)	0.244
				3	−46.2 (1.8)	166.3 (2.9)	0.065
				4	−22.8 (1.9)	−159.0 (0.7)	0.023

Sidechains of residues A2 and A4				
N_2 inversion	State	Pop.	State	Pop.
residue A2	1	0.602	2	0.398
residue A4	1	0.783	2	0.217

Dihedral	State	χ	Pop.	State	χ	Pop.	State	χ	Pop.
χ_2 (A2)	1	104.8 (2.8)	0.929	2	129.4 (3.2)	0.035	3	159.3 (0.3)	0.036
χ_2 (A4)	1	100.4 (3.4)	0.993	2	125.8 (0.5)	0.004	3	158.3 (0.3)	0.003
χ_3 (A2)	g	75.6 (2.4)	0.115	t	180.0 (8.7)	0.581	g′	−52.9 (1.9)	0.304
χ_3 (A4)	g	88.4 (5.4)	0.052	t	−174.7 (7.0)	0.863	g′	−53.5 (1.6)	0.085
χ_5 (A2)	g	59.1 (1.9)	0.898	t	178.9 (1.3)	0.085	g′	−75.8 (0.2)	0.017
χ_5 (A4)	g	58.6 (2.4)	0.554	t	−178.6 (2.0)	0.428	g′	−76.8 (0.5)	0.018
χ_6 (A2)	g	81.0 (0.4)	0.016	t	−179.5 (3.1)	0.984			
χ_6 (A4)	g	85.1 (9.0)	0.047	t	178.9 (7.8)	0.953			

shows that the molecular flexibility decreases as the chain length increases, the sequence of states A1–U1 being preponderant in the polymer. We note that the regular sequence of states $(A1–U1)_n$ corresponds to a nearly 2_1 helix ($\varphi_h = 167°$, $h = 9.02$ Å, shown in Fig. 4). The regular structure $(A1–U2)_n$ is a 3_1 helix ($\varphi_h = 121°$, $h = 8.78$ Å), less stable by 1.82 kcal/mol per dimer.

Calculations of the solvation free energy.—As already mentioned, all the above results were obtained by using dielectric constant 3.0 in the calculation of the Coulomb energy; such a value was chosen, in analogy with previous work [9–11], in order to simulate the screening of electrostatic interactions by the solvent molecules. The next step was a more realistic account of the solvent effects, i.e. the evaluation of the solvation free energy, for the smaller oligomers, using the procedure described in the previous section. In these calculations the solvation free energy ΔG is added to the total strain energy of the isolated molecule, computed with dielectric constant 1, for consistency with the use of atomic charges in the computation of ΔG_{solv}. Thus, for each structure the atomic coordinates stored after energy minimization were re-used to compute ΔG_{solv} and E_{Coul} (without further minimization).

Table 6
Conformer populations for the central U–A–U residues in heptamer **UAUAUAU**

Main chain U–A				A–U			
State	φ	ψ	Pop.	State	φ	ψ	Pop.
1	39.6 (2.5)	15.7 (1.1)	0.898	1	−26.9 (1.1)	−38.6 (1.2)	0.908
2	20.7 (2.3)	−39.8 (1.1)	0.102	2	−18.7 (3.5)	53.3 (3.4)	0.008
				3	−43.9 (1.6)	171.3 (3.4)	0.036
				4	−21.6 (1.6)	−157.2 (0.8)	0.048

Sidechains of the central **A** residue									
N_2 inversion		State	Pop.		State	Pop.			
		1	0.681		2	0.319			
Dihedral	State	χ	Pop.	State	χ	Pop.	State	χ	Pop.
χ_2	t	103.3 (2.3)	0.969	2	127.2 (0.8)	0.016	3	158.6 (0.1)	0.015
χ_3	g	85.9 (2.4)	0.085	t	177.2 (7.0)	0.737	g′	−53.9 (1.5)	0.178
χ_5	g	59.9 (1.7)	0.754	t	178.7 (1.1)	0.229	g′	−76.4 (0.2)	0.017
χ_6	g	82.3 (1.4)	0.011	t	179.6 (3.6)	0.989			

Dimers. Such a procedure was used to re-compute the whole (φ; ψ) maps for both **UA** and **AU**, and the sidechain statistics was repeated for the two dimers with inclusion of the solvation free energy. Inspection of the maps showed that this treatment of the solvent effect does not change the locations of energy minima significantly, except that in **AU** solvation brings up a fifth minimum at about (−45, −50°): such a conformation (indicated as A1* in Tables 3 and 4) had also been found in the trimers, but it can be excluded from the statistics owing to its rather high energy. The results, listed in Table 7, indicate a stabilization of minimum U2 in **UA**, while in the case of **AU** solvation yields an appreciable population of states A2 and A3, in comparison with the preponderance of state A1 computed on the basis of $\epsilon = 3$. The last column of Table 7 shows that accounting of the allowed sidechain conformers has only slight effects on the (φ; ψ) state populations.

Trimers and pentamer. Also all previous conformers of trimers **UAU** and **AUA** and selected conformers of pentamer **UAUAU** were considered for the treatment including hydration. Again, the results of these computations indicate a stabilization of state U2 and of states A2 and A3 relatively to U1 and A1, respectively, in comparison with the

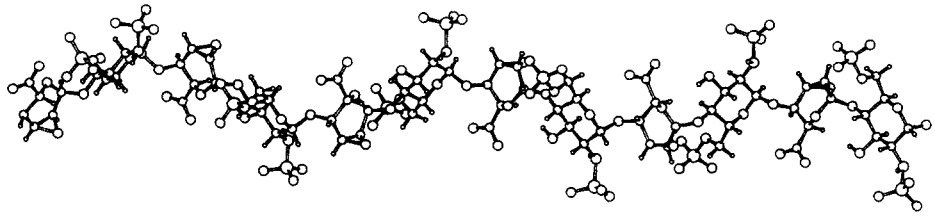

Fig. 4. Lowest-energy helical conformation of heparin epoxide.

Table 7
Solvent effect on dimers **UA** and **AU**. Relative values of energies of isolated molecule (calculated with $\epsilon = 1$), solvation energies, and total energies, compared with the values computed for the isolated molecule with $\epsilon = 3$. (Energies expressed in kcal/mol.) Populations computed at 25°C on the basis of the relative energies (P_0) and by averaging over the sidechain conformations (P_1)

No solvent			Solvent			
State	ΔE_{isol} ($\epsilon = 3$)	ΔE_{isol} ($\epsilon = 1$)	ΔG_{solv}	ΔE_{tot}	P_0	P_1
Dimer **UA**						
U1	0.17	2.24	0.94	2.65	0.011	0.013
U2	0.00	0.00	0.53	0.00	0.978	0.986
U3	1.95	3.22	0.00	2.69	0.010	0.001
U4	2.49	2.80	2.68	4.95	0.001	0.000
Dimer **AU**						
A1	0.00	0.14	0.79	0.00	0.457	0.610
A2	1.60	1.38	0.00	0.45	0.214	0.155
A3	1.48	0.00	1.20	0.27	0.289	0.200
A4	1.50	1.17	1.20	1.44	0.040	0.035

computations without solvent, confirming the trend found in Table 7. However, here the differences in solvation energy among the various conformers reach as much as 10 kcal/mol: the reliability of these large differences, arising mainly from the quadrupole term, seems questionable. Indeed, the theory of the continuum model of solvent utilized here is based on the assumption of a spherical cavity of solvent; hence, a molecule with an elongated shape, such as our oligomers, probably does not fit to this approximation. For these reasons we cannot attempt to modify the statistics presented in Table 6 on the basis of a quantitative account of solvation, although there are indications that it leads to a greater flexibility of the polymer chain.

Analysis of interproton distances.—Any comparison with experimental data would require, in principle, the full modeling of a polymer chain or a statistical approach. As a qualitative interpretation of interproton distances deduced from nOe measurements, we preliminarily computed the same distances in the lowest-energy structures of the **AU** and **UA** dimers; since a few of them were in disagreement with respect to the experimental ones, all conformers have been recomputed to yield non-minimized (φ; ψ) inter-residue distance maps: the latter were then overimposed to the previously computed energy maps (Fig. 3). Although the reliability of this procedure is questionable, as the geometry of the rings and side chains were kept fixed, it was apparent that quite a few regions enclosed by iso-curves corresponding to the experimental distances were too far off the energy minima.

A more detailed study has been then made on all energy-minimized conformers of the **UAU** trimer, where all nearest-neighboring inter-residue interactions are found. Here all possible values for side-chain and glycosidic linkage torsions were used as initial points. The results are reported in Table 8, where the shortest distance found by calculation (d_{min}) and the relative energy are also reported: again, while experimental distances A(6)–U(1) and A(1)–U(3) may be reproduced with a modest energy cost (< 2 kcal/mol), a few short contacts measured from nOe [e.g. A(6)–U(4)] do not correspond

Table 8
Comparison between experimental proton–proton inter-residue distances (Å), derived from the nOe values observed for the polymer and those computed in trimer **UAU** (the lowest value found in any of the minimum-energy conformers). Associated energies are in kcal/mol

Protons	Exptl	Computed	(ΔE)	d_{min} [a]	(ΔE)
A(1)–U(3)	2.0	2.26	0.0	2.10	1.98
A(1)–U(4)	2.3	2.38	0.0		
A(4)–U(1)	2.3	2.28	0.0		
A(5)–U(1)	3.0	3.88	0.0	3.04	2.63
A(5)–U(4)	2.7	2.79	1.91		
A(6)–U(1)	2.4	3.98	0.0	2.34	1.47
A(6′)–U(1)	3.3		0.0		
A(6)–U(2)	3.0	4.59	0.0	2.53	2.95
A(6)–U(4)	2.3	3.30	2.31	3.26	2.32

[a] Shortest distances computed in other conformers (within 3 kcal/mol).

to any energy-allowed conformation; discrepancies may be ascribed to the use of an isotropic model in interpreting experimental nOe data (a few of them are not fully reliable also because of signal overposition).

4. Conclusions

The conformational characteristics of the oligomers of heparin epoxide have been exhaustively analyzed by means of molecular mechanics. The basic information is given by the (φ; ψ) energy maps for the two dimers computed with $\epsilon = 3$ in the absence of solvent, both of which present four minima within 2 kcal/mol, suggesting a considerable flexibility of the polymer chain (mainly corresponding to different values of the ψ dihedral angle). However, extensive calculations on higher oligomers, where also solvation effects were neglected, show an increasing restriction on the allowed conformations as the chain grows, due to combined effects of steric and electrostatic interactions: states U3 and U4 are forbidden at all from the trimers on, while states U1 and A1 appear preponderant in a long chain. On the other hand, the solvation free energy, computed according to the continuum model [13,14], stabilizes states U2, A2 and A3 both in dimers and in trimers. Thus, although we could not quantitatively evaluate the effect of solvation on the conformation of higher oligomers, the present picture of the heparin epoxide chain indicates the possible presence of two conformers for the U–A linkage and three conformers for the A–U linkage, in qualitative agreement with the chain flexibility proposed by Hricovíni et al. in the preceding article. It is conceivable that in the near future a molecular dynamics study including water molecules explicitly may lead to more quantitative conclusions. The possible equilibrium between the $^{5}H_{0}$ and $^{0}H_{5}$ ring forms of the epoxide unit should also be considered. Such a work could also clarify some serious discrepancies between observed and calculated interproton distances.

Acknowledgements

One of us (J.G.) has been supported by Alfa Wassermann S.p.A. Drawing of molecular structures was accomplished with the SCHAKAL program [19], as adapted by M.R.

References

[1] O. Jardetzky, *Biochim. Biophys. Acta*, 621 (1980) 227–232.
[2] S. Piani, B. Casu, E.G. Marchi, G. Torri, and F. Ungarelli, *J. Carbohydr. Chem.*, 12 (1993) 507–521.
[3] M. Jaseja, R.N. Rej, F. Sauriol, and A.S. Perlin, *Can. J. Chem.*, 67 (1989) 1449–1456.
[4] R. Tiozzo, M.R. Cingi, D. Reggiani, T. Andreoli, S. Calandra, M.R. Milani, S. Piani, E.G. Marchi, and M. Barbanti, *Thrombosis Res.*, 70 (1993) 99–106.
[5] B.L. Podlogar and D.J. Raber, *J. Org. Chem.*, 54 (1989) 5032–5035.
[6] N.L. Allinger and Y.H. Yu, *QCPE*, 13 (1981) 395.
[7] J.W. Krajewski, P. Gluziñski, Z.U. Lipkowska, A. Banaszek, L. Párkányi, and A. Kálmán, *Carbohydr. Res.*, 144 (1985) 13–22.
[8] D.R. Ferro and M. Ragazzi, CHAMP: *Conformational (Hyper) Analysis Milan Package*, Istituto di Chimica delle Macromolecole del CNR, Milano, Italy, 1993.
[9] M. Ragazzi, D.R. Ferro, and A. Provasoli, *J. Comput. Chem.*, 7 (1986) 105–112.
[10] D.R. Ferro, A. Provasoli, M. Ragazzi, G. Torri, B. Casu, G. Gatti, J.-C. Jaquinet, P. Sinaij, M. Petitou, and J. Choay, *J. Am. Chem. Soc.*, 108 (1986) 6773–6778.
[11] M. Ragazzi, D.R. Ferro, B. Perly, P. Sinaij, M. Petitou, and J. Choay, *Carbohydr. Res.*, 195 (1990) 169–185.
[12] D.R. Ferro, P. Pumilia, A. Cassinari, and M. Ragazzi, *Int. J. Biol. Macrom.*, 17 (1995) 131–136.
[13] I. Tvaroška and T. Kozár, *J. Am. Chem. Soc.*, 102 (1980) 6929–6936.
[14] I. Tvaroška, *Biopolymers*, 21 (1982) 1887–1897.
[15] I. Tvaroška, in G. Naray-Szabo (Ed.), *Theoretical Chemistry of Biological Systems*, Elsevier, Amsterdam, 1986, pp 283–348.
[16] A.D. Buckingham, *Physical Chemistry, An Advanced Treatise*, Vol. IV, Academic Press, New York, 1970.
[17] A.A. Rashin and B. Honig, *J. Phys. Chem.*, 89 (1985) 5588–5593.
[18] N. Rej and A.S. Perlin, *Carbohydr. Res.*, 200 (1990) 437–447.
[19] E. Keller, *Chem. Unserer Zeit*, 14 (1980) 56–60.